

CuO and CeO₂ catalysts supported on Al₂O₃, ZrO₂, and SiO₂ in the oxidation of CO at low temperature

Gonzalo Águila, Francisco Gracia, Paulo Araya*

Centro para la Investigación Interdisciplinaria Avanzada en Ciencias de los Materiales, Departamento de Ingeniería Química y Biotecnología, Universidad de Chile, Casilla 2777, Santiago, Chile

ABSTRACT

The effect of the support, Al₂O₃, ZrO₂, and SiO₂, on the activity for CO oxidation of a series of CuO and CeO₂ monometallic and bimetallic catalysts was studied. The catalysts were prepared by coimpregnation of the support with the adequate amount of Cu and Ce nitrates to obtain a loading of 2% Cu and/or 8% Ce. It was found that the support has a strong influence on the activity of the different bimetallic catalysts. Interestingly, the SiO₂ supported catalyst shows the higher activity. The bimetallic supported catalysts follow the activity sequence CuO–CeO₂/SiO₂ > CuO–CeO₂/ZrO₂ > CuO–CeO₂/Al₂O₃. In the absence of CeO₂, the most active monometallic catalyst was the CuO/ZrO₂ system. The different degree of interaction between CuO and CeO₂ particles, induced by the support, can explain the activity results for the bimetallic catalysts.

Keywords:

Al₂O₃
SiO₂
ZrO₂
Copper
CeO₂
CO oxidation

1. Introduction

The oxidation of CO to CO₂ is a very important reaction from the standpoint of environmental control. Although this reaction is traditionally carried out on supported noble metals, it has been well known for many years that transition metals, particularly Cu, are also very good catalysts for it [1].

In recent years, and moved by the need to remove CO from the feed stream of fuel cells, there has been renewed interest in this reaction, and numerous papers have been published on the selective oxidation of CO with O₂ in the presence of large amounts of H₂ (PROX reaction). Different catalytic systems have been studied for this reaction, among them those based on noble metals [2–6], Au [7–10], and transition metals, especially copper-based catalysts [11–22]. The greater activity of Cu compared to that of other transition metals like Co, Ni, Cr, and Zn has been reported recently by Mariño et al. [15], confirming that it is one of the best candidates for replacing the noble metals.

The most widely studied catalysts based on copper for the PROX reaction include CeO₂ as a component, and can be classified into three kinds: (i) CuO and CeO₂ catalysts [11–16], (ii) CuO catalysts doped with CeO₂ (or vice versa) supported on alumina [17–20],

and (iii) CuO catalysts supported on mixed Ce_xZr_(1-x)O₂ oxides [21,22].

It is well known that the CuO–CeO₂ system has excellent activity in the oxidation of CO [23], even higher than that of the noble metals [24], so it is not strange that a large part of the publications on the PROX reaction are related to the CuO–CeO₂ system. The ease of the Ce(III)–Ce(IV) redox cycle and the high mobility of oxygen in the crystal structure are two important properties of CeO₂. As a result of that, these oxides are capable of “adsorbing” oxygen reversibly [25], a property that is used in catalytic converters of automobiles as a source of oxygen when the effluent from the engine has a reducing nature [26]. The high activity of the CuO–CeO₂ system is attributed to the strong interaction between Cu nanoparticles and the CeO₂ support. This interaction causes the reduction of the support and of the small CuO clusters to occur at low temperature [24,27]. In this way, adsorption of CO produces an easy reduction of the catalyst’s surface with the generation of CO₂ at low temperature. A mechanism that involves redox processes of the sites at the CuO–CeO₂ interface and also involves the presence of O₂[–] as an intermediary was proposed some years ago by Martínez-Arias et al. [28] for the oxidation of CO with O₂ over a CuO/CeO₂ catalyst. The mechanism involves reduction and adsorption of CO on the interface sites and reoxidation of the surface by O₂ from the gas phase in a Mars Van Krevelen type mechanism. Recently, the same author [29] showed that reduction of the surface of a CuO/CeO₂

* Corresponding author. Tel.: +56 2 9784284; fax: +56 2 6991084.
E-mail address: arayap@cec.uchile.cl (P. Araya).

catalyst starts at the interfacial CuO–CeO₂ positions, followed by reduction of CuO, and finally reduction of the rest of the CeO₂ that is not in contact with the copper oxide.

Although the binary CuO–CeO₂ catalysts show good performance in the PROX reaction, several studies have been made in parallel with the purpose of improving their efficiency and stability, incorporating other components, either as activity promoters or simply as supports.

In the case of the CuO–CeO₂ system supported on Al₂O₃, the studies have shown that the addition of CeO₂ increases considerably the activity of Cu supported on alumina [18–20]. The kind of species formed by cerium oxide supported on alumina has been studied, among others, by Martínez-Arias et al. [30]. They studied various ceria samples (loadings between 1% and 39%) on alumina (200 m²/g). The cerium species found on the alumina surface are mainly highly dispersed CeO₂ crystalline aggregates of a two-dimensional (2D) and three-dimensional (3D) type. The presence of different CeO₂ species on the alumina surface produces, as expected, differences in the Cu activity in CuO–CeO₂ catalysts supported on alumina, as shown in a previous report by Martínez-Arias et al. [31]. The results obtained show that the copper species in contact with the 3D CeO₂ species are reduced easily at temperatures below 100 °C, and they would be responsible for the high activity of the CuO–CeO₂/Al₂O₃ catalysts.

Several years ago Fornasiero et al. [32] found that the mixed CeO₂–ZrO₂ oxides with a Ce/Zr mole ratio equal to one had far better redox properties than those of the separate oxides. Thus, the incorporation of zirconia results in a highly efficient Ce⁴⁺ ↔ Ce³⁺ cycle at moderate temperatures. Considering that oxidation of CO on CuO–CeO₂ involves the reduction of both CuO and the support, it was believed that CuO/CeZrO₂ catalysts could be even more active than CuO/CeO₂ catalysts [28]. The results, however, showed that this hypothesis was not fulfilled, and that the best catalyst was the binary CuO/CeO₂ system both in the absence [28] and in the presence of H₂ [21,22].

It seems clear, then, that the presence of zirconia does not favor the activity of the CuO–CeO₂ catalysts. However, it must be kept in mind that in these studies the zirconia and ceria form a solid solution on which the CuO is supported. The situation may be different if the system is prepared so that the characteristics of the CuO–CeO₂ and CuO–ZrO₂ binary systems are potentiated, as it is well known that Cu supported on ZrO₂ is a very active catalyst for CO oxidation with O₂ [33–35].

Considering the above, the objective of this work was to study the effect of different supports on the activity of the CuO–CeO₂ system. As a first approximation, the study was carried out in the absence of H₂, and Al₂O₃, ZrO₂, and SiO₂ were considered as supports. To our best knowledge, the effect of SiO₂ on the activity of the CuO–CeO₂ system has not been studied previously, and it was included due to its well-known inert character. It is expected that the CuO and CeO₂ species formed on SiO₂ should be different from those formed on ZrO₂ and Al₂O₃, where it is known that there is an important interaction between the Cu species and the support. The loading, 2% Cu and 8% Ce, was chosen considering the work of Park et al. [17], who reported those concentrations as optimal for the CuO–CeO₂/Al₂O₃ system, but obviously this is one of the variables that will be studied in later work on SiO₂ and ZrO₂ supports.

2. Experimental

The catalysts were prepared by coimpregnation of the support with a solution containing Cu and Ce nitrates, with a total loading of 2% Cu and 8% Ce. They were then dried at 105 °C overnight and calcined at 500 °C for 3 h in a muffle furnace. The supports used were ZrO₂, obtained by calcination at 700 °C for 3 h of anhydrous

zirconium supplied by MEI; Al₂O₃ was obtained by grinding agglomerated γ -alumina (BASF) and separating the fraction smaller than 100 mesh, and Aerosil 200 (Degussa) was used directly as a source of silicon oxide. Furthermore, a catalyst with 2% Cu supported on CeO₂ was prepared. Cerium oxide was obtained by calcination of cerium nitrate at 550 °C for 4 h, and it was then impregnated with a solution of copper nitrate and subjected to the same drying and calcination treatment described above.

The characterization of the supports and catalysts included N₂ sorptometry, XRD, Raman spectroscopy, and temperature programmed reduction with H₂ (TPR).

Determination of the BET specific area by N₂ sorptometry was made on Micromeritics ASAP 2010 equipment after degassing the sample at 200 °C. The crystal structure of the different catalysts and supports was determined on a Siemens D-5000 diffractometer using Cu K α radiation and a scan rate of 0.02°/min.

Raman spectroscopy was performed with a Renishaw Microscope System RM1000 using an Argon ion laser as an illumination source (514.5 nm) and CCD detector electrically cooled. The Raman equipment was coupled to a LECA microscope (50 \times magnifications) and the collection optics was used in the backscattering configuration. The laser power was in the 1.0–3.0 mW to prevent heating of the sample.

Finally, the TPR analysis was made on conventional equipment with a TCD detector at a flow of 20 cm³/min of a 5% H₂/Ar mixture and a heating ramp of 10 °C/min.

The kinetics tests were made in a piston flow tubular reactor, with a current of 2% CO and 3% O₂ at a total flow rate of 100 cm³/min. After loading the reactor with 0.2 g of catalyst, the sample was pretreated at 300 °C for 1 h in O₂, and the reactor was cooled to room temperature. The reactants were then fed and the temperature was increased at a rate of 3 °C/min, taking samples every 20 °C to determine the concentration of CO, O₂, and CO₂ on a PerkinElmer Autosystem chromatograph with a CTR column (Alltech) and a TCD detector.

3. Results and discussion

3.1. Characterization of the solids

3.1.1. N₂ sorptometry

The results of the physical characterization of supports and catalysts by N₂ sorptometry are shown in Table 1. It is seen that the specific area does not vary significantly when impregnating the cerium and copper oxides on ZrO₂ and SiO₂. When Al₂O₃ was used as support a slight decrease was seen in the catalyst's area, in agreement with literature reports [36]. Among the three supports used, ZrO₂ is the one that has the smallest specific area, but as will be shown below, it is still capable of dispersing a substantial amount of copper on its surface due to a strong interaction between the Cu species and the support.

3.1.2. XRD analysis

The results of the XRD analysis of the catalysts supported on Al₂O₃, ZrO₂, and SiO₂, as well as those of the pure supports, are shown in Fig. 1(A–C), respectively. Fig. 1(D) shows the XRD spectra of the pure CeO₂ support and of the CuO/CeO₂ catalyst prepared on that support. All the figures include the principal diffraction lines of the cerium and copper oxides as reference.

In Fig. 1(A) it is seen that when Al₂O₃ is used as support, none of the catalysts that contain Cu show the diffraction peaks of bulk CuO, indicating that in all the catalysts the Cu is highly dispersed on the support. This is not strange considering that the limit above which bulk CuO is formed is approximately 4% Cu for every 100 m²/g of Al₂O₃ [37,38]. Therefore, since in our case the Cu

Table 1
Physical characterization of the catalysts

Sample	BET surface area (m ² /g)	CeO ₂ particle size (nm) ^a
Al ₂ O ₃ support		
Al ₂ O ₃	208	
2%Cu/Al ₂ O ₃	210	
8%Ce/Al ₂ O ₃	181	8.7
2%Cu8%Ce/Al ₂ O ₃	174	7.1
ZrO ₂ support		
ZrO ₂	32	
2%Cu/ZrO ₂	33	
8%Ce/ZrO ₂	33	-
2%Cu8%Ce/ZrO ₂	32	-
SiO ₂ support		
SiO ₂	195	
2%Cu/SiO ₂	196	
8%Ce/SiO ₂	198	9.0
2%Cu8%Ce/SiO ₂	182	7.6
CeO ₂ support		
CeO ₂	87	
2%Cu/CeO ₂	79	10.2

^a Estimated by XRD using the (1 1 1) face.

loading capacity was only 2% on an alumina of 200 m²/g, the dispersion capacity of alumina has not been surpassed, and the Cu should be expected to be highly dispersed, forming a structure of the Cu aluminate type [37].

In the case of the catalysts that contain cerium oxide, CeO₂/Al₂O₃ and CuO–CeO₂/Al₂O₃, the characteristic peaks of crystalline CeO₂ are clearly seen, in agreement with literature reports [19]. The particle size of CeO₂ in these catalysts, estimated by XRD, is 8.7 and 7.1 nm, respectively, as shown in Table 1. These values agree quite well with those reported by Martínez-Arias et al. [31], who found CeO₂ particle between 8 and 10 nm for the same systems.

The XRD spectra of the catalysts supported on ZrO₂ are shown in Fig. 1(B). Analysis of the different catalysts shows that the peaks of the support dominate the XRD spectrum, making very difficult the direct observation of peaks corresponding to CuO and CeO₂ because they overlap those of the support. For that reason a detailed analysis of those spectra will not be made. However, analysis of the spectrum of the pure support shows the peaks corresponding to a mixture of monoclinic and tetragonal zirconia, whose proportions have already been calculated in a previous work, and correspond to 83% monoclinic and 17% tetragonal [39]. The particle size of CeO₂ is not reported in Table 1 because of the problems mentioned above.

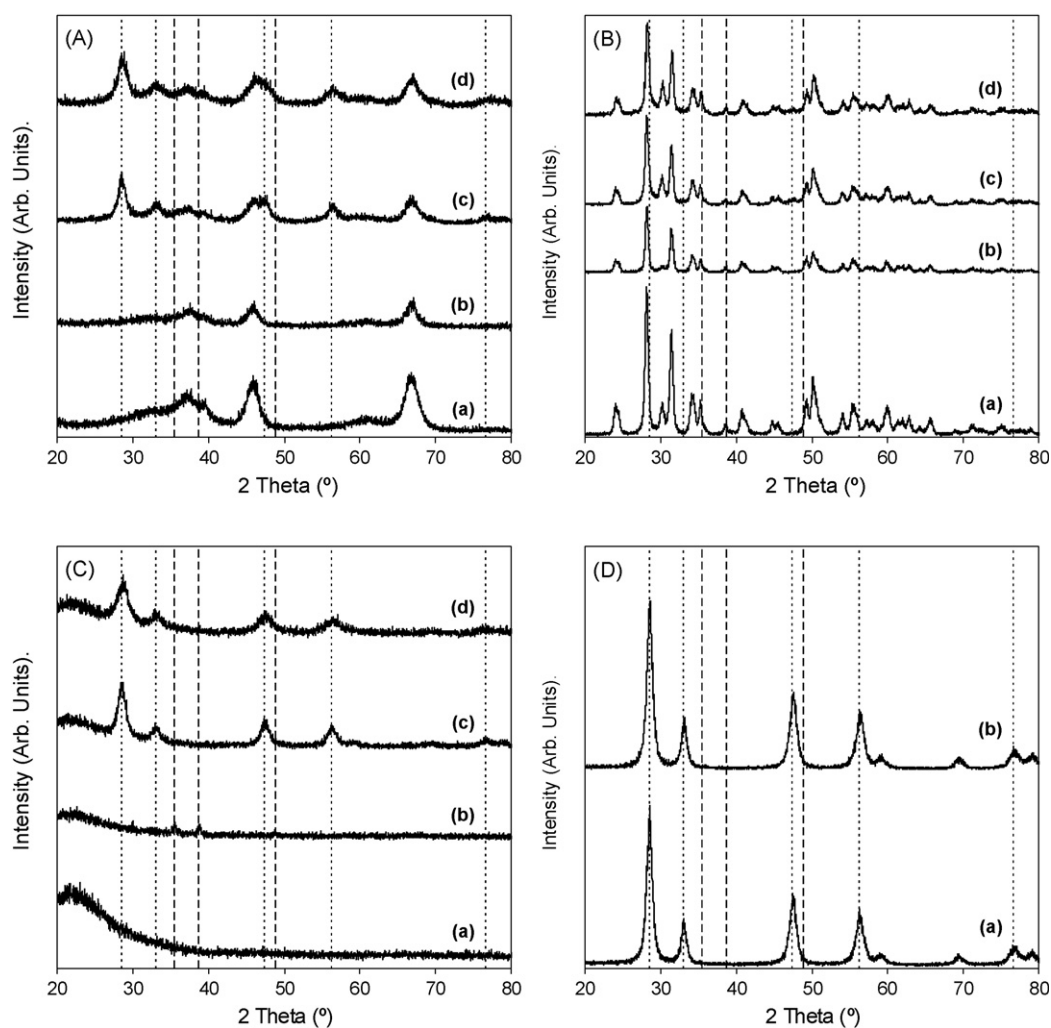


Fig. 1. XRD patterns of various catalysts and supports. (A) Al₂O₃ support: (curve a) pure Al₂O₃; (curve b) CuO/Al₂O₃; (curve c) CeO₂/Al₂O₃; (curve d) CuO–CeO₂/Al₂O₃. (B) ZrO₂ support: (curve a) pure ZrO₂; (curve b) CuO/ZrO₂; (curve c) CeO₂/ZrO₂; (curve d) CuO–CeO₂/ZrO₂. (C) SiO₂ support: (curve a) pure SiO₂; (curve b) CuO/SiO₂; (curve c) CeO₂/SiO₂; (curve d) CuO–CeO₂/SiO₂. (D) CeO₂ support: (curve a) pure CeO₂; (curve b) CuO/CeO₂. The characteristic peaks of CuO (---) and CeO₂ (· · · ·) are included as reference.

The XRD spectra of the catalysts supported on SiO₂ are shown in Fig. 1(C). It is seen that the spectrum of the CuO/SiO₂ catalyst shows the peaks characteristic of bulk CuO at 35.5° and 38.7°. The formation of bulk CuO on silica, even at Cu loadings smaller than 2%, was reported previously [40], and it indicates the low interaction between the support and the Cu oxide.

The CeO₂/SiO₂ catalyst shows the peaks attributed to CeO₂, which are also seen in the CuO–CeO₂/SiO₂ catalyst. However, as seen in Table 1, the size of the cerium oxide particles supported on SiO₂ decreases from 9.0 to 7.6 nm when both oxides are present on the surface of the silica. Although the size of the CeO₂ particles does not vary substantially when Cu and Ce are coimpregnated, the effect on the size of the CuO particles is more important. In fact, the peaks corresponding to CuO, which appear in the CuO/SiO₂ catalyst, are no longer seen in the CuO–CeO₂/SiO₂ catalyst. This suggests that the simultaneous impregnation of Cu and Ce nitrates favors a high dispersion of CuO with a particle size not detectable by XRD. A similar effect has been reported by Xiaoyuan et al. [41] for CuO–CeO₂ catalysts supported on Al₂O₃ using high copper loadings (10% Cu). Obviously, this effect is not seen with our catalysts supported on alumina, because due to the low copper loading used no bulk CuO is formed on alumina.

Finally, the XRD diagrams of the CeO₂ support and the 2% CuO/CeO₂ catalyst, which are presented in Fig. 1(D), shows the

characteristic peaks of the fluorite type structure of CeO₂. According to literature reports [15,36,42], at that copper loading crystalline CuO is not detected in the CuO/CeO₂ catalyst, indicating that this species is highly dispersed on the cerium oxide. According to Hu et al. [36], crystalline CuO is seen at loadings greater than 4.9% Cu on a cerium oxide of 58 m²/g, so it cannot be expected to see crystalline CuO in our catalyst, which has 2% Cu on a cerium oxide with an area greater than 80 m²/g.

3.1.3. Raman analysis

The Raman spectra of the catalysts supported on alumina, zirconia and silica are shown in Fig. 2(A–C), while the spectra of cerium oxide and of the copper catalyst supported on that oxide are shown in Fig. 2(D).

As seen in Fig. 2(A), in the case of the CuO/Al₂O₃ catalyst there are no peaks around 290, 340 and 630 cm⁻¹ attributed to bulk CuO [43–45], indicating that CuO is highly dispersed over the support, in agreement with the XRD results.

The CeO₂/Al₂O₃ and CuO–CeO₂/Al₂O₃ catalysts show clearly the CeO₂ peak at 460 cm⁻¹ corresponding to the triply degenerate F_{2g} mode of fluorite CeO₂ [16,46]. In the CuO–CeO₂/Al₂O₃ catalyst the peak corresponding to CeO₂ remains practically in the same place, but there is an additional wide peak at about 620 cm⁻¹. The appearance of a peak around 600 cm⁻¹ has been reported by

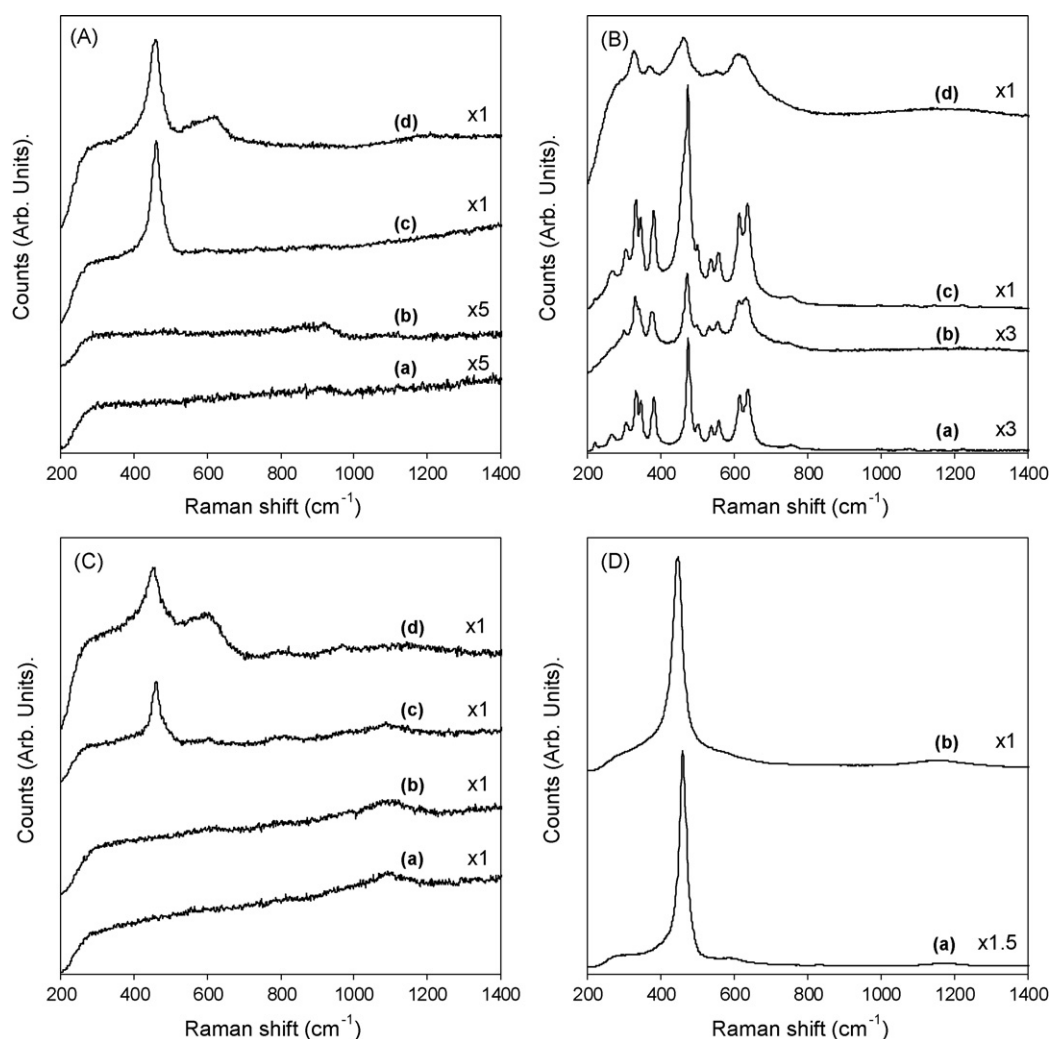


Fig. 2. Raman spectra of various catalysts and supports. (A) Al₂O₃ support: (curve a) pure Al₂O₃; (curve b) CuO/Al₂O₃; (curve c) CeO₂/Al₂O₃; (curve d) CuO–CeO₂/Al₂O₃. (B) ZrO₂ support: (curve a) pure ZrO₂; (curve b) CuO/ZrO₂; (curve c) CeO₂/ZrO₂; (curve d) CuO–CeO₂/ZrO₂. (C) SiO₂ support: (curve a) pure SiO₂; (curve b) CuO/SiO₂; (curve c) CeO₂/SiO₂; (curve d) CuO–CeO₂/SiO₂. (D) CeO₂ support: (curve a) pure CeO₂; (curve b) CuO/CeO₂.

Martínez-Arias et al. [46] in CeO₂ supported CuO catalysts, and it is attributed to the formation of oxygen vacancies generated by the incorporation of Cu²⁺ in the structure of CeO₂. The appearance of a peak around 620 cm⁻¹ in the CuO–CeO₂/Al₂O₃ catalyst suggests, therefore, that coimpregnation of both oxides on the surface of alumina favors a close interaction between the copper and cerium species that would allow the incorporation of copper ions in the structure of cerium oxide, giving rise to oxygen vacancies in a similar manner to that when CuO is supported on CeO₂. The existence of this interaction between highly dispersed CuO and the CeO₂ particles on the surface of alumina has been proposed, among others, by Martínez-Arias et al. [31], and it is responsible for the substantial increase in activity when CeO₂ is added to CuO/Al₂O₃ catalysts [18–20]. Therefore, our Raman results perfectly agree with what has been reported in the literature. On the other hand, no peaks attributable to bulk CuO are seen in this catalyst, in agreement with the XRD results, suggesting a high dispersion of the copper oxide species.

The Raman spectra of the catalysts based on ZrO₂ are shown in Fig. 2(B). In the case of the pure support, the bands corresponding to monoclinic zirconia are clearly seen at 333, 377, 475, and 559 cm⁻¹, as reported by Pokrovski et al. [47], together with some lower intensity bands corresponding to tetragonal ZrO₂ at 265, 313, and 640 cm⁻¹ [48,49], in agreement with the presence of both crystalline phases found by XRD. In the case of the CuO/ZrO₂ catalyst some small bands appear at 290, 340 and 630 cm⁻¹ that may be attributed to bulk CuO. However, a shift to lower frequencies and a widening of all the bands attributable to ZrO₂ are seen, making it difficult to clearly assign those bands to the presence of bulk CuO. This shift and widening of the bands corresponding to the support suggests the existence of an important interaction between the CuO and the support.

On the contrary, in the CeO₂/ZrO₂ catalyst the bands of the support remain practically unchanged, indicating that CeO₂ and ZrO₂ do not interact substantially. In fact, the only difference between the spectra of the support and the CeO₂/ZrO₂ catalyst is the appearance of a shoulder at 460 cm⁻¹ that can be attributed to the peak of the fluorite type structure of CeO₂. The appearance of this peak confirms the existence of CeO₂ particles, something that cannot be done with the XRD spectrum of that catalyst.

In the case of the CuO–CeO₂/ZrO₂ catalyst, the spectrum of the support undergoes even greater changes compared to CuO alone supported on ZrO₂. In fact, this spectrum shows the disappearance or overlapping of bands due to the support with considerable displacement of their maxima, pointing to a strong interaction between the CuO species and ZrO₂. This catalyst does not show any bands that can be attributed with certainty to bulk CuO.

The Raman spectra of the CuO/SiO₂, CeO₂/SiO₂ and CuO–CeO₂/SiO₂ catalysts are very similar to those obtained when alumina was used as support, and they are included in Fig. 2(C). In agreement with the previous results of XRD, for the CuO/SiO₂, a small band can be observed at 630 cm⁻¹, which correspond to CuO bulk [43–45]. The Raman spectrum of the CeO₂/SiO₂ catalyst shows the band attributed to CeO₂ at practically the same frequency as that seen with Al₂O₃ at 460 cm⁻¹. When copper and cerium were coimpregnated, however, the cerium oxide band was displaced to shorter wavelengths, around 454 cm⁻¹, and a second peak again appears centered at 600 cm⁻¹. As already mentioned, this peak is attributed to the generation of vacancies in the CeO₂ structure due to the incorporation of Cu, pointing to the existence of close contact between the oxides of copper and cerium on the surface of the support. It can therefore, be assumed that the ceria particles and the highly dispersed copper oxide clusters interact on the silica surface in a similar manner to that seen when both oxides are supported on Al₂O₃. This hypothesis is confirmed by the TPR experiments discussed below.

Finally, Fig. 2(D) shows that the spectrum of pure CeO₂ shows the characteristic band at 460 cm⁻¹ corresponding to the triply degenerate F_{2g} mode of fluorite CeO₂ [16,46]. When CuO is supported on its surface, the band is shifted to 445 cm⁻¹. This shift is greater than that seen with the supported CuO–CeO₂ catalysts, reflecting the strong CuO–CeO₂ interaction when CuO is deposited directly on the CeO₂. This was expected because ideally all the CuO can interact with the CeO₂. Additionally, it should be noted that the CuO–CeO₂/Al₂O₃ catalyst does not show an important displacement of the band assigned to CeO₂, indicating a smaller interaction between CuO and CeO₂ on the surface of Al₂O₃ compared to that of the ZrO₂ and SiO₂ supports. On the other hand, no bands attributable to CuO are seen, in agreement with the XRD results, and it can therefore, be assumed that the CuO is highly dispersed on the surface of CeO₂.

3.1.4. TPR analysis

The results of the TPR experiments with the catalysts based on Al₂O₃, ZrO₂ and SiO₂ are shown in Fig. 3(A–C), respectively. Fig. 3(D) shows the TPR corresponding to pure CeO₂ and to CuO supported on CeO₂. Table 2 shows the H₂ consumption of the different catalysts during the TPR experiments.

As can be seen in Fig. 3(A), the CuO/Al₂O₃ catalyst has a wide reduction peak that starts at about 260 °C, with a maximum close to 320 °C. This peak has been attributed by Dow and Huang [33] to the reduction of highly dispersed Cu, forming a Cu aluminate type species on the surface of the alumina [37]. The formation of this species accounts for the high reduction temperature seen in the TPR experiment. As seen in Table 2, the consumption of H₂ by the CuO/Al₂O₃ catalyst (5.4×10^{-5} mol of H₂) is the lowest of the three supported CuO catalysts, and it is lower than that expected for the complete reduction of CuO (6.2×10^{-5} mol of H₂), in agreement with the observation of Severino et al. [50] with catalysts having low copper loadings on alumina.

In the case of the CeO₂/Al₂O₃ catalyst, it is seen that the CeO₂ is not substantially reduced below 380 °C, in agreement with the literature [18,19]. Above that temperature a poorly defined H₂ consumption spectrum is seen to extend above 650 °C. Cheekta-marla et al. [18] reported reduction peaks of CeO₂ supported on alumina at 520 and 730 °C, attributed to the reduction of surface oxygen anions (Ce⁴⁺ to Ce³⁺) and bulk CeO₂, respectively. The shape of the TPR spectrum of Fig. 3(A) does not allow a clear distinction of those peaks, and it must therefore, include the reduction of the surface oxygen species at low temperatures and the reduction of bulk oxygen at higher temperatures. The consumption of H₂ by this catalyst up to 650 °C is 2.8×10^{-5} mol and as discussed below, this confirms the reduction of surface oxygen and bulk CeO₂.

On the other hand, the CuO–CeO₂/Al₂O₃ catalyst shows a first reduction peak with a maximum around 220 °C, followed by a series of poorly defined peaks, without H₂ consumption returning to zero before 650 °C. Xiaoyuan et al. [41] observed a shift of the maximum corresponding to the CuO reduction peak from 310 to 250 °C when CeO₂ is added to a CuO/Al₂O₃ catalyst. Therefore, that first peak can be associated to the reduction of the Cu species interacting with CeO₂ on the surface of the alumina. The higher temperature reduction peaks can be assigned to the reduction of Cu species not interacting with CeO₂ and to the reduction of CeO₂, because the presence of CuO makes the reduction of CeO₂ to occur at significantly lower temperatures [18], causing an overlapping of peaks with those associated with the reduction of the Cu species. The increased ease for the reduction of CuO in the presence of CeO₂ has been observed both in the CuO–CeO₂ system [12,24,42,51] and in systems containing both oxides supported on alumina [17,19,31]. As proposed by Park et al. [19], the fact that in the CuO–CeO₂/Al₂O₃ catalyst the CuO is reduced at a lower tempera-

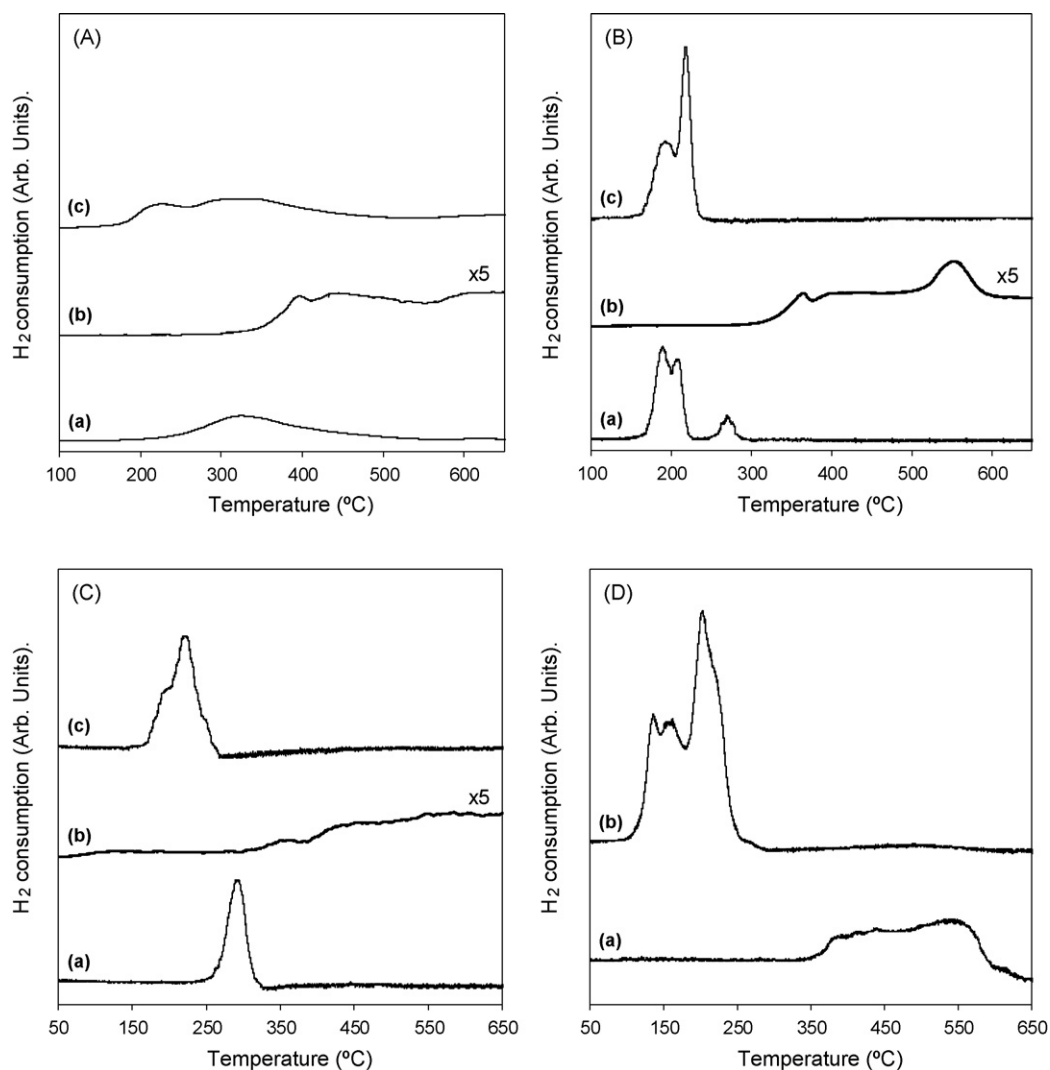


Fig. 3. TPR of various catalysts and supports. (A) Al_2O_3 support: (curve a) $\text{CuO}/\text{Al}_2\text{O}_3$; (curve b) $\text{CeO}_2/\text{Al}_2\text{O}_3$; (curve c) $\text{CuO-CeO}_2/\text{Al}_2\text{O}_3$. (B) ZrO_2 support: (curve a) CuO/ZrO_2 ; (curve b) $\text{CeO}_2/\text{ZrO}_2$; (curve c) $\text{CuO-CeO}_2/\text{ZrO}_2$. (C) SiO_2 support: (curve a) CuO/SiO_2 ; (curve b) $\text{CeO}_2/\text{SiO}_2$; (curve c) $\text{CuO-CeO}_2/\text{SiO}_2$. (D) CeO_2 support: (curve a) pure CeO_2 ; (curve b) CuO/CeO_2 .

ture is a clear indication that both oxides are in close contact on the surface of the alumina. A similar conclusion was reached by Martínez-Arias et al. [31] using other characterization techniques like EPR and FTIR of CO adsorbed on the surface of $\text{CuO-CeO}_2/$

Al_2O_3 . Therefore, the results of the TPR experiments as well as the Raman spectrum of this catalyst point to the existence of an important interaction between the copper and cerium species on the surface of the alumina.

The TPR spectra of the materials supported on ZrO_2 , presented in Fig. 3(B), show the strong influence of the support on the reducibility of the oxides supported on its surface. The reduction spectrum of CuO supported on ZrO_2 shows three reduction peaks. According to the literature, those at the lowest temperature originate from the reduction of highly dispersed (at atomic level) Cu species, while the small higher temperature peak (around 270°C) originates from the reduction of species of the bulk CuO type [34,35,52]. The appearance of a small amount of bulk CuO is expected because the capacity of zirconium oxide to disperse copper is similar to that of alumina, and is about 4.5% of Cu per $100\text{ m}^2/\text{g}$ [40]. Since $32\text{ m}^2/\text{g}$ zirconium oxide was used, a 2% Cu loading is above that limit (1.4% Cu for a $32\text{-m}^2/\text{g}$ support). As shown in Table 2, this catalyst's H_2 consumption is equivalent to an almost complete reduction of CuO to Cu^0 within the temperature range of ambient to 300°C , in agreement with what was found by Manzoli et al. [22] for this kind of system.

In the case of the Ce oxide catalyst supported on ZrO_2 , Fig. 3(B) shows a wide H_2 consumption peak that starts around 330°C and extends above 650°C , with a well-defined maximum at 550°C . In

Table 2

H_2 consumption by the different catalysts and supports

Sample	H_2 consumed $\times 10^5$ (mol)
Al_2O_3 support	
2% $\text{Cu}/\text{Al}_2\text{O}_3$	5.4
8% $\text{Ce}/\text{Al}_2\text{O}_3$	2.8
2% $\text{Cu}8\%\text{Ce}/\text{Al}_2\text{O}_3$	8.3
ZrO_2 support	
2% Cu/ZrO_2	6.4
8% Ce/ZrO_2	2.8
2% $\text{Cu}8\%\text{Ce}/\text{ZrO}_2$	8.9
SiO_2 support	
2% Cu/SiO_2	6.6
8% Ce/SiO_2	2.6
2% $\text{Cu}8\%\text{Ce}/\text{SiO}_2$	9.0
CeO_2 support	
CeO_2	13.8
2% Cu/CeO_2	21.6

principle, this peak should correspond to the reduction of surface oxygen of CeO₂, whose maximum has been reported between 520 [18] and 570 °C [42]. The initial temperature of the CeO₂ reduction peak is similar to that found in the case of CeO₂/Al₂O₃, and total H₂ consumption, shown in Table 2, is also similar in both cases. Fornasiero et al. [32] found that the introduction of ZrO₂ in the structure of cerium oxide facilitates the reduction of ceria. It can be speculated, therefore, that supporting CeO₂ on ZrO₂ may lead to a type of interaction that favors the reduction of cerium oxide, but it is not possible to state that this also happens with our catalyst.

In the case of the CuO–CeO₂/ZrO₂ catalyst only two reduction peaks are seen. The one corresponding to bulk CuO seen with the CuO/ZrO₂ catalyst disappears in this catalyst, and even more interesting is the complete disappearance of peaks attributable to the reduction of CeO₂ at temperatures higher than 250 °C. The disappearance of the bulk CuO peak can be attributed to a greater CuO dispersion in this catalyst, a phenomenon that, as mentioned above, has been reported in the case of CuO–CeO₂/Al₂O₃. The disappearance of the reduction peaks of CeO₂ above 250 °C can only be accounted for by the reduction of these species at temperatures below that value. In fact, Table 2 shows that in this catalyst H₂ consumption is 8.9×10^{-5} mol of H₂, similar to that seen in the case of CuO–CeO₂/Al₂O₃, and obviously higher than that expected from the reduction of 100% of the CuO present in the catalyst. Both reduction peaks found with this catalyst can be interpreted, therefore, as the reduction of highly dispersed CuO (lowest temperature peak) and the reduction of CeO₂ (highest temperature peak). It can, therefore, be concluded that the reducibility of CeO₂ when CuO is present on the surface of the support is better using ZrO₂ instead of Al₂O₃ as support.

The TPR spectra of the catalysts supported on SiO₂, shown in Fig. 3(C), confirm once again the strong influence of the support on the reducibility of the copper and ceria species on its surface. For the CuO/SiO₂ catalyst there is only one reduction peak centered at 280 °C, attributed to the reduction of bulk CuO [34,52]. As seen in Table 2, the consumption of H₂ occurs in the temperature range from ambient to 325 °C, and it is that needed for the complete reduction of bulk CuO.

With the CeO₂/SiO₂ catalyst there is a wide peak that starts around 320 °C and may be attributed to the reduction of oxygen on the surface of CeO₂, followed by the reduction of part of the bulk CeO₂, as has been proposed in the literature [27,41]. The H₂ consumption with this catalyst, as shown in Table 2, is somewhat lower than that found for CeO₂ catalysts supported on alumina and zirconia, but as will be seen below, it must also include the reduction of part of the bulk CeO₂.

In the case of the CuO–CeO₂/SiO₂ catalyst, two peaks are seen with apparent maxima at 180–220 °C attributed to the reduction of small CuO clusters with and without interaction with CeO₂, respectively [see [20] and refs. therein]. Since bulk CuO particles are no longer detectable by XRD, it can be stated that coimpregnation of the precursors of Cu and Ce induces greater dispersion of Cu on the silica, as has been reported by Cheekatamarla et al. [18], among others, for the CuO–CeO₂/Al₂O₃ system. In a similar manner to what happens with the CuO–CeO₂/ZrO₂ catalyst, in this catalyst the peaks attributable to the reduction of CeO₂ at temperatures above 250 °C cannot be detected. Considering that the H₂ consumption of 8.9×10^{-5} is similar to that of the previous cases, and that it cannot be explained by the reduction of CuO, it is evident that the reduction of CeO₂ occurs at a very low temperature in this catalyst due to the effect of the presence of CuO on its surface. This fact points to a very effective interaction between CuO and CeO₂ on this support.

Finally, Fig. 3(D) shows the TPR spectra of the CeO₂ support and the 2%Cu/CeO₂ catalyst. In the case of CeO₂ a wide reduction peak is

seen starting around 360 °C and returning to the baseline at 600 °C. This peak has been assigned to the reduction of surface oxygen from CeO₂ [27,42]. The reduction of bulk oxygen with pure CeO₂ occurs at higher temperatures than those considered in this study. The H₂ consumption by this catalyst (see Table 2) is 13.8×10^{-5} mol. Considering the specific area of CeO₂ (87 m²/g) and the mass loaded in the reactor (0.2 g), a consumption of 7.9×10^{-6} mol of H₂ per m² of CeO₂ is obtained. This value agrees quite well with that reported by Zimmer et al. [53] of 9.5 ± 1.4 μmol of H₂ per m² for undoped CeO₂. The figure also shows the spectrum of the copper catalyst supported on this cerium oxide. At least four reduction peaks are seen with maxima at 140, 160, 205 and 230 °C. The last three peaks are very similar to those reported by Avgouropoulos and Ioannides [12], who identify them as peaks α, β1 and β2. They suggest that the α peak corresponds to the reduction of copper ions interacting strongly with CeO₂, while peaks β1 and β2 would correspond to larger CuO particles, less associated with CeO₂. Liu and Flytzani-Stephanopoulos [54] report that the CuO clusters interacting strongly with CeO₂ are reduced in the 125–175 °C range, while the peaks at 140 °C and 160 °C can also be assigned to the reduction of these kinds of species, possibly to the stepwise reduction Cu²⁺ → Cu¹⁺ → Cu⁰ [27,53]. In any case, it is important to point out that this catalyst has reduction peaks at lower temperatures than any of the other catalysts.

Comparison of the TPR spectrum of unsupported cerium oxide with the TPR spectra of the cerium oxides supported on Al₂O₃, ZrO₂, and SiO₂ allows some interesting conclusions to be reached. In all the supported CeO₂ catalysts the reduction of the CeO₂ particles starts at a lower temperature than when they are not supported, and it extends beyond 650 °C. In the case of pure CeO₂ the consumption of H₂ drops to zero around 600 °C, indicating the end of the reduction of the surface oxygen species. The H₂ consumption of below 650 °C shown by the supported CeO₂ catalysts, reported in Table 2, can only be partially attributed to the reduction of the surface oxygen species, and must include the reduction of other CeO₂ species. In fact, if we multiply the H₂ consumption of pure CeO₂, 7.9×10^{-6} mol of H₂/m² of CeO₂, by the exposed surface area of a supported CeO₂ catalyst, we get an expected H₂ consumption of 1.4×10^{-5} mol. From this calculation it is assumed that the specific area of the supported CeO₂ particles is similar to that of pure CeO₂, in agreement with the particle sizes reported in Table 1. In all the supported CeO₂ catalysts, H₂ consumption up to 650 °C is between 2.6×10^{-5} mol and 2.8×10^{-5} mol, clearly indicating the reduction of other species in addition to surface oxygen. These species can correspond to 2D particles of CeO₂ not detected in the estimation of particle size by XRD, or to the reduction of part of bulk CeO₂ at lower temperature. More work is needed to elucidate the origin of this overconsumption of H₂ with the supported CeO₂ catalysts.

Therefore, the information from previous characterization analyses can be summarized by stating that CuO is highly dispersed in all the systems except CuO/SiO₂, where the peaks of crystalline CuO are clearly discernible by XRD. On the other hand, CeO₂, or at least an important part of it, is found as relatively large particles with 3D structure, because in all the systems that contain CeO₂ the particles are clearly identifiable by XRD and Raman. Also, the TPR experiments show that in all the systems the presence of CeO₂ facilitates reduction and increases the dispersion of the Cu species on the surface of the catalysts. The most easily reduced Cu species, due to the presence of CeO₂, appear when using SiO₂ and ZrO₂ as support. In these catalysts it is also seen that the effect of copper on the reducibility of CeO₂ is greater than in the case of using alumina as support, causing the cerium oxide to be reduced at significantly lower temperatures. These results suggest that the CuO–CeO₂ interaction is more effective on the ZrO₂ and SiO₂ supports than on Al₂O₃. As will be seen below, the difference

in the reducibility of the Cu and Ce species on the surface of the catalysts agrees very well with the difference in the catalytic activity shown by these systems.

3.2. Catalytic activity of the different systems

The results of CO oxidation activity as a function of temperature of the catalysts supported on Al_2O_3 , ZrO_2 and SiO_2 are shown in Fig. 4, which also shows the activity of cerium oxide and of the CuO catalyst supported on that oxide. It is seen that cerium oxide has a relatively low activity, either as the pure oxide or supported on Al_2O_3 , ZrO_2 or SiO_2 , achieving conversions around 3% at 200 °C. In relation to supported CuO catalysts, their behavior is strongly dependent on the support used. While the $\text{CuO}/\text{Al}_2\text{O}_3$ and CuO/SiO_2 catalysts are also very slightly active in this temperature range, not exceeding 5% conversion at 200 °C, the CuO supported on ZrO_2 catalyst achieves conversions close to 95% at 200 °C. The low activity of the $\text{CuO}/\text{Al}_2\text{O}_3$ and CuO/SiO_2 catalysts can be attributed to different reasons. In the case of the catalyst supported on alumina, the low activity can be associated with the formation of a copper species of the aluminite type [37] that is difficult to reduce and has lower catalytic activity in the oxidation of CO than the highly dispersed CuO clusters that are formed on alumina at greater copper loadings [55,56]. In the case of copper supported on SiO_2 , and due to the inert character of this support, the particles become agglomerated, forming bulk type CuO, even at low copper loadings, as shown by the TPR and XRD spectra. These bulk type CuO particles are reduced at relatively high temperatures and, in agreement with Severino and Laine [55], they have low activity for the oxidation of CO per unit of copper mass.

The high activity of the CuO supported on ZrO_2 catalyst compared to that of CuO supported on Al_2O_3 has been reported by Zhou et al. [35] and Dow and Huang [33] for copper oxide catalysts supported on zirconia stabilized with yttrium. While Zhou et al. [35] attribute the high activity of CuO/ZrO_2 to the ease of the $\text{Cu}^{2+} \rightarrow \text{Cu}^{1+} \rightarrow \text{Cu}^{2+}$ redox cycle and to the ease of desorption of the oxygen species on the surface of the catalyst, Dow and Huang [57] highlight the role of oxygen vacancies on the CO oxidation activity of CuO supported on ZrO_2 stabilized with yttrium. In our case the high activity of the CuO/ZrO_2 catalyst correlates very well with the greater ease of reduction of the CuO species highly dispersed on ZrO_2 compared to the reducibility of the copper

species supported on alumina and silica, as seen in the TPR spectra of Fig. 3.

As shown in Fig. 4, the effect of the addition of CeO_2 to the supported CuO catalyst is dependent on the support used, although it is always beneficial to the catalyst's activity. When alumina is used as the support, and as expected from the literature reports [17,18,20,31], the addition of CeO_2 produces a substantial increase in the catalyst's activity compared to copper supported on alumina. In fact, whereas $\text{CuO}/\text{Al}_2\text{O}_3$ has an activity lower than a 4% at 180 °C, the $\text{CuO-CeO}_2/\text{Al}_2\text{O}_3$ catalyst achieves 95% at the same temperature. The high activity of the $\text{CuO-CeO}_2/\text{Al}_2\text{O}_3$ catalyst correlates well with the increased reducibility of the CuO species seen in the TPR experiments. As proposed by Martínez-Arias et al. [31], the greater reduction ease of the Cu species interacting with ceria on the surface of alumina favors the catalytic activity in the oxidation of CO. These sites at the CuO-CeO_2 interface are responsible for both the initiation of the catalyst's reduction process with CO [29] and the high activity of the catalyst by facilitating the redox cycle in the presence of CO and O_2 [46].

The increased activity of CuO by addition of CeO_2 is also seen when ZrO_2 is used as support, but due to the high activity of the CuO/ZrO_2 catalyst the effect is less dramatic than in the case of using alumina as support. In fact, the conversion versus temperature curve of the $\text{CuO-CeO}_2/\text{ZrO}_2$ catalyst shifts by about 50–60 °C to lower temperatures than that of the CuO/ZrO_2 catalyst. The $\text{CuO-CeO}_2/\text{ZrO}_2$ catalyst has a conversion of 95% at 140 °C, while the CuO/ZrO_2 catalyst achieves the same conversion at 200 °C. It should be pointed out that the activity of the $\text{CuO-CeO}_2/\text{ZrO}_2$ catalyst is quite higher than that of the $\text{CuO-CeO}_2/\text{Al}_2\text{O}_3$ catalyst. Therefore, the use of ZrO_2 as support appears as an interesting alternative to be compared with alumina, which is frequently used as support for CuO and CeO_2 .

The largest increase in the activity of CuO by the addition of CeO_2 is produced in the catalyst supported on SiO_2 . As shown in Fig. 4, the CuO/SiO_2 catalyst does not have a measurable activity at temperatures below 180 °C. In contrast, the $\text{CuO-CeO}_2/\text{SiO}_2$ catalyst shows activity even at 40 °C, and it increases suddenly its conversion with temperature between 80 and 100 °C, achieving almost complete conversion at 130 °C. This makes the $\text{CuO-CeO}_2/\text{SiO}_2$ catalyst the most active one in the series of CuO-CeO_2 supported catalysts. Martínez-Arias et al. [31,50] found that cerium oxide on alumina is found as 2D and 3D particles, and they suggest that the Cu in contact with the 3D CeO_2 particles is responsible for the high activity of the $\text{CuO-CeO}_2/\text{Al}_2\text{O}_3$ catalysts [30]. Since it is known that silica is an inert support, it seems reasonable to assume that the particles of CeO_2 interact weakly with the support and form preferentially 3D particles. It can therefore be postulated that the high activity of the $\text{CuO-CeO}_2/\text{SiO}_2$ catalyst can be accounted for by the presence on its surface of highly dispersed Cu and CeO_2 forming preferentially 3D particles.

In any case, the two most active catalysts, $\text{CuO-CeO}_2/\text{SiO}_2$ and $\text{CuO-CeO}_2/\text{ZrO}_2$, are also those that present the most efficient interaction between the CuO and the CeO_2 on its surface, as seen in the TPR experiments. Therefore, the high activity of these catalysts correlates well with the increased reducibility of the CuO and CeO_2 species on the surface of those supports.

Finally, it is interesting to note that although the activity of all the supported CuO-CeO_2 catalysts presented in this study is lower than that of a catalyst having the same amount of copper supported directly on CeO_2 , as seen in Fig. 4, the activity of the catalysts supported on SiO_2 and ZrO_2 is quite close to that of the CuO/CeO_2 catalyst, particularly at temperatures above 100 °C. This indicates that the interaction between CuO and CeO_2 on the surface of these supports, though not as effective as that achieved by supporting CuO directly on CeO_2 , is sufficiently important to

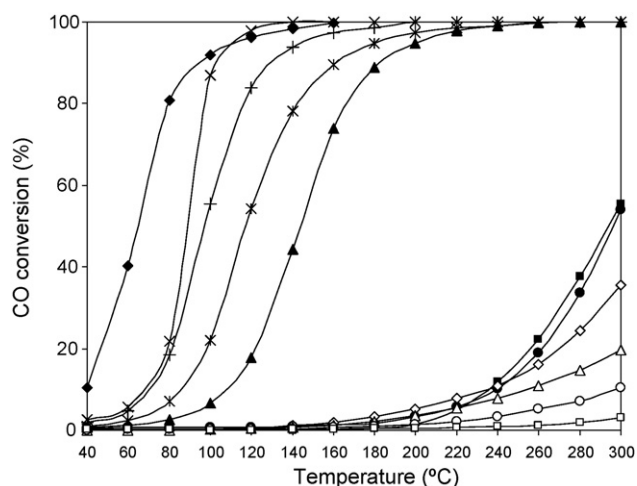


Fig. 4. CO conversion vs. reactor temperature for various catalysts and supports. (◆) CuO/CeO_2 ; (×) $\text{CuO-CeO}_2/\text{SiO}_2$; (+) $\text{CuO-CeO}_2/\text{ZrO}_2$; (*) $\text{CuO-CeO}_2/\text{Al}_2\text{O}_3$; (▲) CuO/ZrO_2 ; (■) CuO/SiO_2 ; (●) $\text{CuO}/\text{Al}_2\text{O}_3$; (◇) pure CeO_2 ; (△) $\text{CeO}_2/\text{ZrO}_2$; (○) $\text{CeO}_2/\text{Al}_2\text{O}_3$; (□) $\text{CeO}_2/\text{SiO}_2$.

generate catalysts having a high CO oxidizing activity. Optimizing the CuO and CeO₂ loading on these supports (ZrO₂ and SiO₂) can improve even more the activity of these catalysts, reducing the difference in activity compared to the CuO/CeO₂ catalyst.

4. Conclusions

The results show that in the three supports used, Al₂O₃, ZrO₂ and SiO₂, the incorporation of CeO₂ on the surface is always beneficial for the catalysts' activity. The most noticeable synergistic effects are seen when using Al₂O₃, and particularly when using SiO₂ as support. The latter seems to potentiate to a greater extent the interaction between highly dispersed Cu and 3D particles of CeO₂, generating the most active catalyst of those studied. The effect of CeO₂ on the activity of copper supported on ZrO₂ is less dramatic than with the other supports, partly due to the high activity exhibited by copper when it is supported on ZrO₂, making the incorporation of CeO₂ increase proportionally less with respect to the activity of the catalyst.

The most active catalysts are obtained by supporting CuO and CeO₂ on SiO₂ and ZrO₂. These catalysts have better activity than those supported on Al₂O₃, which is commonly reported as support in the literature. Clearly, these systems are worthy of being explored more deeply. The definition of total loading, and the optimum relation between Cu/Ce using ZrO₂ and SiO₂ as supports are aspects that will be investigated in later work.

Acknowledgements

This work was financed under Fondecyt Project 1070961. The donation of hydrous zirconia by Magnesium Elektron Inc. MEI (USA) is gratefully acknowledged.

References

- [1] J. Kummer, *Prog. Energy Combustion Sci.* 6 (1980) 177.
- [2] D. Suh, C. Kwak, J. Kim, S. Kwon, T. Park, *J. Power Sources* 142 (2005) 70.
- [3] S. Ito, H. Tanaka, Y. Minemura, S. Kameoka, K. Tomoshige, K. Kunimori, *Appl. Catal. A* 273 (2004) 295.
- [4] F. Mariño, C. Descorme, D. Duprez, *Appl. Catal. B* 54 (2004) 59.
- [5] H. Tanaka, S. Ito, S. Kameoka, K. Tomishige, K. Kunimori, *Appl. Catal. A* 250 (2003) 255.
- [6] H. Tanaka, S. Ito, S. Kameoka, K. Tomishige, K. Kunimori, *Catal. Commun.* 4 (2003) 1.
- [7] G. Avgoropoulos, T. Ioannides, C. Papadopoulou, J. Batista, S. Hocevar, H. Matralis, *Catal. Today* 75 (2002) 157.
- [8] R. Torres, A. Ueda, K. Tanaka, M. Haruta, *J. Catal.* 168 (1997) 125.
- [9] H. Oh, J. Yang, C. Costello, Y. Wang, S. Bare, H. Kung, M. Kung, *J. Catal.* 210 (2002) 375.
- [10] R. Grisel, B. Nieuwenhuys, *J. Catal.* 199 (2001) 48.
- [11] G. Sedmark, S. Hocevar, J. Levec, *J. Catal.* 222 (2004) 87.
- [12] G. Avgoropoulos, T. Ioannides, *Appl. Catal. A* 244 (2003) 155.
- [13] G. Sedmark, S. Hocevar, J. Levec, *J. Catal.* 213 (2003) 135.
- [14] Y. Liu, Q. Fu, M. Stephanopoulos, *Catal. Today* 93 (2004) 241.
- [15] F. Mariño, C. Descorme, D. Duprez, *Appl. Catal. B* 58 (2005) 175.
- [16] G. Marbán, A. Fuertes, *Appl. Catal. B* 57 (2005) 43.
- [17] J. Park, J. Jeong, W. Yoon, H. Jung, H. Lee, D. Lee, Y. Park, Y. Rhee, *Appl. Catal. A* 274 (2004) 25.
- [18] P. Cheektamarla, W. Epling, A. Lane, *J. Power Sources* 147 (2005) 178.
- [19] J. Park, J. Jeong, W. Yoon, C. Kim, D. Lee, D. Lee, Y. Park, Y. Rhee, *Int. J. Hydrogen Energy* 30 (2005) 209.
- [20] C. Shiau, M. Ma, C. Chuang, *Appl. Catal. A* 301 (2006) 89.
- [21] P. Ratnasamy, D. Srinivas, C. Satyanarayana, P. Manikandan, R. Kumaran, M. Sachin, V. Shetti, *J. Catal.* 221 (2004) 455.
- [22] M. Manzoli, R. Di Monte, F. Boccuzzi, S. Coluccia, J. Kaspar, *Appl. Catal. B* 61 (2005) 192.
- [23] W. Liu, M. Flytzani-Stephanopoulos, *J. Catal.* 153 (1995) 304.
- [24] Kundakovic, M. Flytzani-Stephanopoulos, *Appl. Catal. A* 171 (1998) 133.
- [25] Y. Madier, C. Descorme, A. Le Govic, D. Duprez, *J. Phys. Chem. B* 103 (1999) 10999.
- [26] J. Thomas, W. Thomas, *Heterogeneous Catalysis*, VCH, Weinheim, Germany, 1997, 577.
- [27] L. Kundakovic, M. Flytzani-Stephanopoulos, *J. Catal.* 179 (1998) 203.
- [28] A. Martínez-Arias, M. Fernández-García, O. Galvez, J. Coronado, J. Anderson, J. Conesa, J. Soria, G. Munuera, *J. Catal.* 195 (2000) 207.
- [29] A. Martínez-Arias, A. Hungria, M. Fernández-García, J. Conesa, J. Munuera, *J. Phys. Chem. B* 108 (2004) 17983.
- [30] A. Martínez-Arias, M. Fernández-García, L. Salamanca, R. Valenzuela, J. Conesa, J. Soria, *J. Phys. Chem. B* 104 (2000) 4038.
- [31] A. Martínez-Arias, R. Cataluña, J. Conesa, J. Soria, *J. Phys. Chem. B* 102 (1998) 809.
- [32] P. Fornasiero, G. Balducci, R. Di Monte, J. Kaspar, V. Sergo, G. Gubitosa, A. Ferrero, M. Graziani, *J. Catal.* 164 (1996) 173.
- [33] W. Dow, T. Huang, *J. Catal.* 147 (1994) 322.
- [34] T. Huang, K. Lee, H. Yang, W. Dow, *Appl. Catal. A* 174 (1998) 199.
- [35] R. Zhou, X. Jiang, J. Mao, X. Zheng, *Appl. Catal. A* 162 (1997) 213.
- [36] Y. Hu, L. Dong, M. Shen, D. Liu, J. Wang, W. Ding, Y. Chen, *Appl. Catal. B* 31 (2001) 61.
- [37] R. Friedman, J. Freeman, *J. Catal.* 55 (1978) 10.
- [38] B. Strohmeier, D. Leyden, R. Field, D. Hercules, *J. Catal.* 94 (1985) 514.
- [39] G. Aguila, S. Guerrero, F. Gracia, P. Araya, *Appl. Catal. A: Gen.* 305 (2006) 219.
- [40] G. Aguila, F. Gracia, J. Cortés, P. Araya, *Appl. Catal. B* 77 (2008) 325.
- [41] J. Xiaoyuan, L. Liping, C. Yingxu, Z. Xiaoming, *J. Mol. Catal. A* 197 (2003) 193.
- [42] J. Xiaoyuan, L. Guanglie, Z. Renxian, M. Jianxin, C. Yu, Z. Xiaoming, *Appl. Surf. Sci.* 173 (2001) 208.
- [43] M. Francisco, V. Mastelaro, P. Nascente, A. Florentino, *J. Phys. Chem. B* 105 (2001) 10515.
- [44] P. Larson, A. Andersson, *J. Catal.* 179 (1998) 72.
- [45] Z. Wang, V. Pischedda, S. Saxena, P. Lazor, *Solid State Commun.* 121 (2002) 275.
- [46] A. Martínez-Arias, D. Gamarra, M. Fernández-García, X. Wang, J. Hanson, J. Rodriguez, *J. Catal.* 240 (2006) 1.
- [47] K. Pokrovski, M. Rhodes, A. Bell, *J. Catal.* 235 (2005) 368.
- [48] V. Sanchez Escribano, E. Fernández López, M. Panizza, C. Resini, J. Gallardo Amores, G. Busca, *Solid State Sci.* 5 (2003) 1369.
- [49] M. Li, Z. Feng, G. Xiong, P. Ying, Q. Xiu, C. Li, *J. Phys. Chem. B* 105 (2001) 8107.
- [50] F. Severino, J. Brito, O. Carías, J. Laine, *J. Catal.* 102 (1986) 172.
- [51] A. Martínez-Arias, M. Fernández-García, J. Soria, J. Conesa, *J. Catal.* 182 (1999) 367.
- [52] Z. Liu, M. Amiridis, Y. Chen, *J. Phys. Chem. B* 109 (2005) 1251.
- [53] P. Zimmer, A. Tschöpe, R. Birringer, *J. Catal.* 205 (2002) 339.
- [54] W. Liu, M. Flytzani-Stephanopoulos, *Chem. Eng. J.* 64 (1996) 283.
- [55] F. Severino, J. Laine, *Ind. Eng. Chem. Prod. Res. Dev.* 22 (1983) 396.
- [56] P. Park, J. Ledford, *Appl. Catal. B: Environ.* 15 (1998) 221.
- [57] W. Dow, T. Huang, *J. Catal.* 160 (1996) 171.